Simulation-Based Design of Drive Mechanism for Flapping Wing Miniature Air Vehicles

A. Ananthanarayanan, W. Bejgerowski, J. Gerdes,
D. Mueller, S.K. Gupta, and S. Wilkerson

Abstract

Flapping wing miniature air vehicles (MAVs) have significant potential in surveillance, search, rescue and reconnaissance applications. These applications require the MAV to carry payloads in the form of batteries, on-board cameras, camera, sensors etc. In order to ensure that the payload capacity of the MAV is maximized for a given wing area and flapping frequency, we need to carefully design the drive mechanism to reduce its mass and ensure that it meets the intended functional requirements. The overall design approach described in this chapter incorporates the advances in modeling and simulations methods in kinematic and dynamic analysis, finite element analysis, and manufacturability analysis. We demonstrate applicability this design approach using two case studies.

9.1   Introduction

Flapping wing miniature air vehicles (MAVs) are expected to present several advantages over conventional MAVs [1-6]. Birds and insects are well known for their high degree of maneuverability and quiet flights. Hence, flapping wing locomotion offers the potential for very stealthy MAVs that are capable of a wide range of flight maneuvers. Flapping wing MAVs can also fly at low forward speeds. These capabilities suggest great potential for usage in indoor operations, surveillance, and urban environments where obstacle avoidance is important.

The following issues need to be addressed for successful realization of flapping wing MAVs in practical applications:

- ***Reduction in Drive Mechanism Weight***: Most applications of flapping wing MAVs require relatively heavy payloads in the form of on-board sensors, batteries, camera, etc. Hence, the overall weight of the MAV needs to be minimized. This also enables longer flight time, which is another fundamental requirement for most flapping wing MAVs. While the payloads generally offer limited potential for weight savings, the drive mechanism that converts the motor's rotary motion into the flapping motion of the wings is a source of weight savings that can be easily controlled by the designer.

- ***High Power Transmission Efficiency***: The rotary motion of the motor is converted into flapping wing motions by the drive mechanism. The strict weight constraint on the MAV makes it beneficial to increase the efficiency of the power transmission and reduce the overall part count of the mechanism.

- ***Low Cost***: In order to make flapping wing MAVs attractive in search, rescue, and recovery efforts, they should be disposable from the cost point of view.

Designing a drive mechanism requires simultaneous consideration to multiple factors. Usually, the primary objective is to minimize the weight of the drive mechanism. The secondary objective is to select the structure shape to minimize the manufacturing cost. The structure shape and size need to ensure that the forces acting on the mechanism do not induce excessive stresses. Furthermore, structure shape and size need to respect manufacturing constraints. In this chapter, an approach for decomposing this challenging problem into more manageable steps will be described and different types of modeling and simulation tools will be presented to perform these steps.

9.2   Simulation-Based Design Framework

The drive mechanism is a critical component of any MAV. The drive mechanism of a MAV must convert the input energy source to the flapping action of the wings using an actuator. Potential forms of input energy are solar energy, wind energy, or simply a DC battery. Typical examples of actuators are DC motors and servo motors. MAVs are usually constructed using the following concept. First, an energy input is supplied to an actuator. Next, the actuator motion is converted to the flapping action of the wing using a drive mechanism. This flapping action of the wings produces lift and thrust forces that sustain MAV flight. The design of the drive mechanism depends on the source of input energy, the actuator used, and the amount of power that has to be transmitted from the actuator to the wings. This section will present a simulation based design framework for realizing the design goal of a MAV drive mechanism,

which converts the input energy to flapping action of the wings. The overall approach for realizing this design goal is illustrated in Figure 9.1..

In the first step, the designer identifies several design concepts for the drive mechanism. These design concepts can be selected from a design repository after performing a feasibility check for the desired flapping action of the MAV, the input energy source and the actuator type to be used.

Subsequently, the design concept suitability has to be evaluated. The mechanism is evaluated based on the power transmission capability of the input energy source, the actuators to be used, and geometric constraints. The mechanism model also depends on the properties of the materials used to realize the mechanism, such as density, structural rigidity etc.
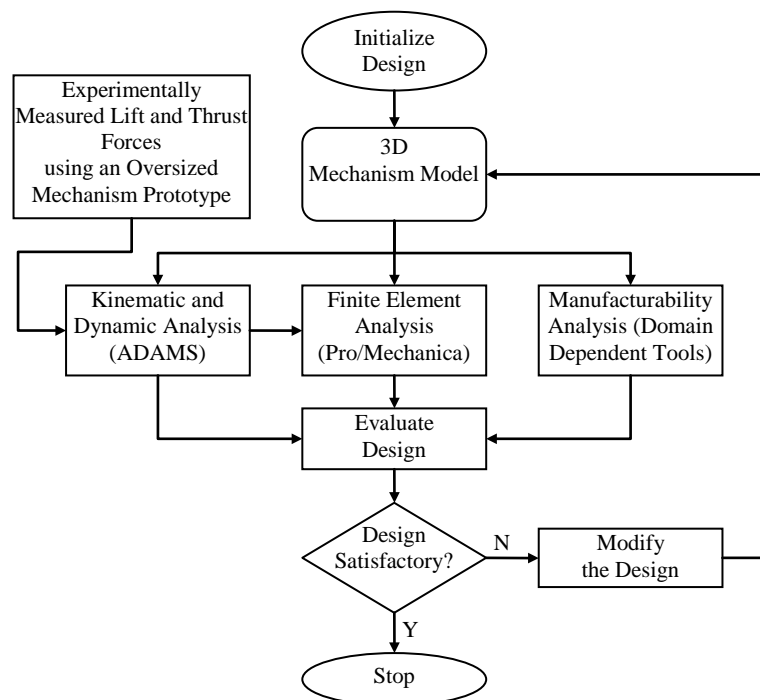

Figure 9.1 Overview of the approach

Currently good computational tools do not exist for estimating lift and thrust force generated by flapping wings. Hence, an oversized and hence safe mechanism prototype need to be used to experimentally measure the lift and thrust forces generated during the flapping motion. The experimentally measured lift and thrust forces are used in a detailed kinematic and dynamic analysis to develop an understanding of the forces acting on the structural members of the

mechanism. Subsequently, the mechanism design is evaluated for performance using finite element analysis to evaluate the stresses on the structural members and manufacturability analysis to impose size constraints on the structural members. The manufacturability analysis on the MAV drive mechanism involves: 1) selection of an appropriate manufacturing process that can be used to fabricate the MAV drive mechanism and 2) development of a detailed manufacturing framework based on the manufacturing constraints.

The final design of the MAV drive mechanism is obtained using an iterative process involving the steps outlined above. The following sections will present two case studies of drive mechanisms, which are used in different versions of MAVs.

9.3   Case Study 1: Design of the Small Bird

In this case study, steps towards creating a MAV platform that weighs less than 15 grams will be described. Figure 9.2 shows the schematic diagram of the drive mechanism concept. Based on the weight, size, and functionality constraints, a compliant mechanism was deemed suitable for realizing the drive mechanism [7-9]. Flexural members were incorporated into the mechanism to provide for distributed compliance in the structure, aiding the flapping motion.
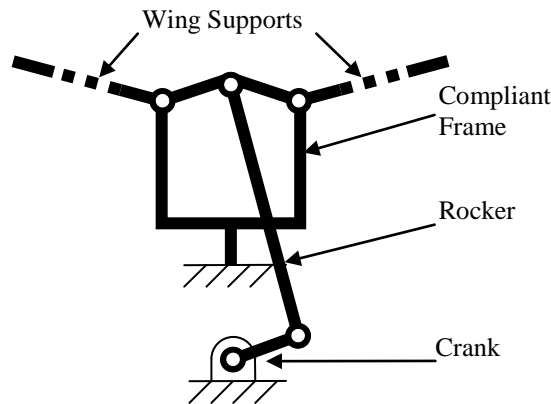
Figure 9.2: Small Bird drive mechanism concept

Due to the weight constraint, a polymer was chosen as the material for the mechanism. Considering the choice of material, the small size scales involved, the shape complexity, and the desire for a scalable manufacturing process, injection molding using multi-piece molds was selected to be the best choice for the manufacturing process [10-17]. Multi-piece molds have multiple mold opening directions. Designing multi-piece molds poses a significant design challenge due to increased mold cost, flash generation, and limited demoldability of the part.

Moreover, the complexity of the part shape and small size scale made it necessary to use multi-gate molds. Placement of gates is a challenging problem, since multiple gates supplying the same cavity in the mold lead to weld-lines on the structure [12, 16]. The weld-line is a molding defect which weakens the part structure [18, 19]. Improper gate positioning may lead to a weld-line being positioned in a structurally demanding region of the part, thereby leading to its failure.

The main decision variables for this problem were therefore part shape, size, parting line locations, gate locations, and sacrificial shape elements. The primary objective function for this problem was the mechanism weight minimization. The secondary objective function for this problem was the minimization of the number of mold pieces. The following three constraints needed to be satisfied. First, the stresses in the structure should not exceed the material limit. Second, the structure shape and size should meet molding process constraints. Finally, the gate placement should ensure the weld-line locations are outside the high stress areas of the structure.

9.3.1 Mechanism Shape Synthesis

The first step in the overall approach was to determine the detailed part shape and dimensions from the concept illustrated in Figure 9.2.

Mechanism shape synthesis can be carried out using the following three step approach. First, to generate the basic shape of the mechanism, the design concept was detailed by adding functionality and moldability constraints. Second, the constrained dimensions of the mechanism were determined by analyzing the mating components and motion requirements. Third, parametric optimization and finite element analysis were utilized to determine the values of the remaining unconstrained critical dimensions.

To obtain the flapping wing action from the rotary input of the motor, a crank-rocker mechanism was designed based on the concept illustrated in Figure 9.2. The motor's rotational velocity is transferred to the crank through a gearbox to reduce the flapping frequency. The crank is connected to a rocker, which displaces the symmetrically placed wing arms. These arms are mounted (pivoted) on the compliant members, which allow for the displacement of the pivoting points, hence feasible mechanism action. Note that without the compliant members, this mechanism concept would be a stationary structure.

Disturbance forces caused by wind gusts during the MAV flight could potentially cause significant out of plane motion of the gears and wing supports on the mechanism. These issues were eliminated by use of a bi-planar design, as shown in Figure 9.3. This design allows for two-point support of several elements in the mechanism. This also constrains the motion of the wing supports to a single vertical plane between the supports. Restriction of out of plane motion is crucial to the mechanism efficiency and therefore, the amount of thrust produced by the wings of the MAV. The bi-planar design also protects the mechanism from impact loads during landings. The area most exposed to impact loads is the lowest point on the frame. Hence the frame should be designed such that it provides an enclosure for the gears.

The issue of wobbling also affects the crank of the mechanism, which transmits the torque from the gear to the rocker. Due to significant forces during flapping motion, the two-point support of its rotation axis is essential.

In order to ensure moldability of the drive mechanism frame, fillets around the shafts were introduced to minimize the differences of the cavity cross-section and allow for better melt flow in the mold. This is shown in Figure 9.3.

After identifying the basic shape of the mechanism using the functionality and moldability constraints, the next step was to determine the dimensions of the mechanism based on functional requirements of the MAV. This was done using the following strategy. First, the fixed and free dimensions of the mechanism were identified. Next, the geometric and dimensional constraints posed by electronic actuators were accounted for. Finally, manufacturing considerations were accounted for before arriving at the final dimensions of the mechanism.

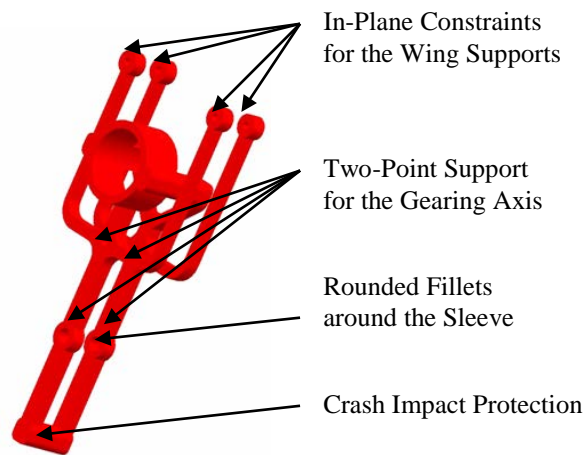Figure 9.4. shows representative dimensions for a mechanism of an MAV.

Figure 9.3: Bi-planar design of the drive mechanism frame

9.3.2 Parametric Optimization

In order to perform structural analysis of the mechanism parts, the forces acting on them have to be estimated. Due to the bi-planar design of the mechanism frame, the out-of-plane forces resulting from the motion were small. Therefore the kinematic modeling was simplified by treating the mechanism as planar.

Due to the distributed compliance of members as a functional characteristic, the drive was modeled as a pseudo-rigid body planar mechanism. The compliant members were modeled as rigid links with torsion springs at anchoring joints.

The sensitivity analysis showed that the influence of the rotational stiffness change on the sought reaction forces is very minor.
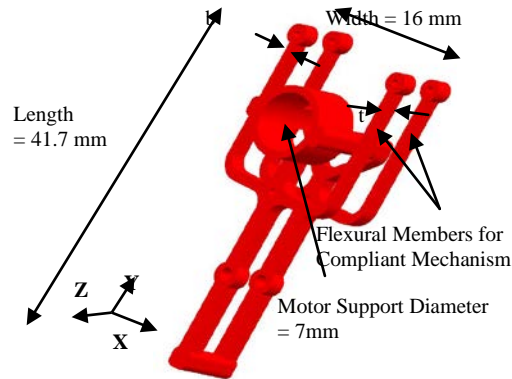

Figure 9.4: Fixed and free dimensions of the mechanism body

Kinematic analysis of the model subsequently revealed the static and dynamic forces on the structural members during the mechanism operation. The inputs into this kinematic analysis were the external forces applied on the mechanism. For this case of the MAV, the two most significant forces are the reaction torque of the motor on the mechanism during its operation, and the external forces on the mechanism due to the wind speed. The reaction torque of the motor can be determined from the manufacturer specifications, while the force due to wind speed has to be obtained experimentally.

A linear test stand was used to measure the thrust and lift of the MAV [20]. When the MAV was attached horizontally to the testing platform, the measured average thrust was 0.077 N and the peak thrust was 0.098 N. The measured peak lift value was 0.150 N.

After constraining the dimensional parameters of the mechanism to accommodate the mechanical and electronic components required for the functionality of the MAV, the remaining critical unconstrained dimensions had to be determined, namely *b* and *t* shown in Figure 9.4. These were assigned by design optimization based on finite element analysis.

The principle idea was to minimize the weight of the mechanism, yet the manufacturing and maximum allowable stresses constraints had to be satisfied. For example, the mold manufacturing constraint required the width *b* of the compliant members to be 0.89 mm.

Finite element analysis of six static maximum load cases was performed and the maximum von Mises stresses were plotted along the structure. The yield

strength of the material was divided by the maximum value of stresses observed by the part to obtain the resulting factor of safety. The frame was designed to have the factory of safety of 1.75. This is an average value recommended for known materials, with certification under reasonably constant environmental conditions, subjected to loads and stresses that can be determined using qualified design procedures. Hence, the depth t of the compliant members was solved to be 1.52 mm.

The finite element analysis also identified the high stress and displacement regions. This is important for recognizing the areas that cannot contain weld-lines, and therefore useful for the gate placement design stage for molding. This will be discussed in further detail in the next section.

9.3.3 Manufacturability Analysis

The first step towards the mold design solution involved determination of the appropriate parting lines, and thereby, the total number of mold pieces, required for molding the mechanism body. For the body frame considered in this case study, the design obtained after incorporating the constraints of the functional requirements, and performing the mechanics-based optimization, consisted of a non-critical shape element for the motor support. Regular polygonal (e.g., triangle, square, and hexagon) and circular shapes were considered for this element. The radius of the maximum circle contained in each shape was kept the same. Two different orientations were tried for each polygon. The first orientation involved a polygon edge aligned with the x-axis. The second orientation was derived by rotating the triangle by 60°, the square by 45°, and the hexagon by 30°. For each shape, the total number of mold pieces, required for molding the part using the steps outlined above, was determined. From this method, the shape of the motor support for minimum number of mold pieces was established to be an inverted triangle.

After optimizing the non-critical shape elements, the mold design consisted of 5 mold pieces and 5 mold side cores. The mold pieces that constituted the mold assembly are shown in Figure 9.5. The demolding process for the part using this mold design is illustrated in Figure 9.6. After obtaining the mold piece design, it has to be checked for part demoldability and flash. After analysis of the part, sacrificial shape elements were added to the part, illustrated in Figure 9.7. Addition of the sacrificial shape element of an appropriate size in the top mold piece ensured that the overall part volume was sufficient to avoid flash and prevent under-filling of the part.

After mold piece design, the next step involved the placement of gates. Gate placement strategy is a very important mold design decision. The location of the gates on the part affects several important parameters, which are: 1) mold cavity filling, 2) warpage in the injection molded part, and 3) location of the weld-lines.
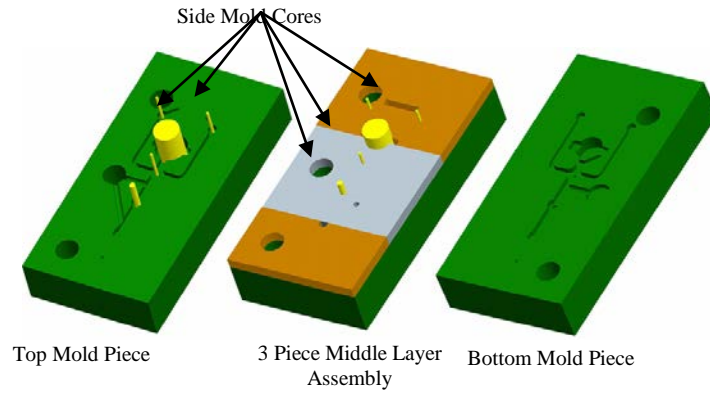
Side Mold Cores

Top Mold Piece   3 Piece Middle Layer   Bottom Mold Piece
                            Assembly

Figure 9.5: Mold design for body-frame fabrication

Step 1:   Step 2:   Step 3:
Removal of Top and Bottom Layer   Removal of Cores   Removal of Middle
of Mold Pieces   Layer Pieces

Step 4:   Final Demolded Part
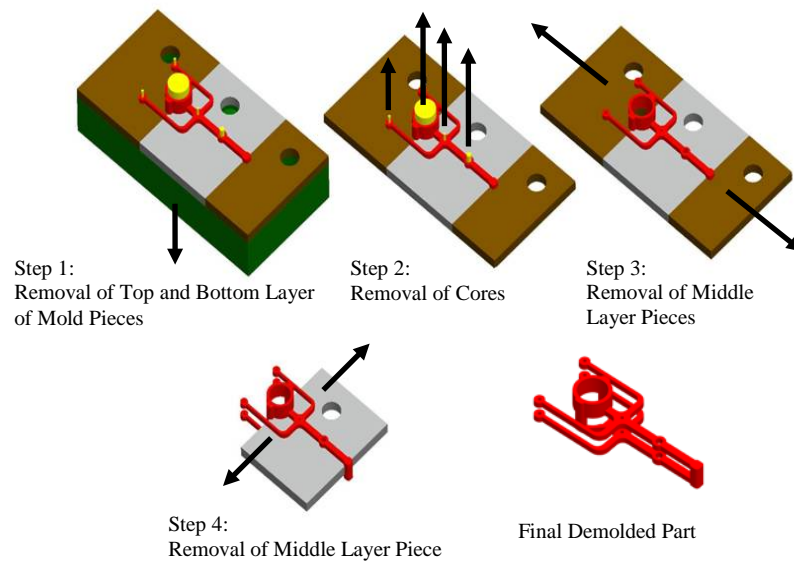Removal of Middle Layer Piece

**Figure 9.6: Parting surface design for in-mold fabrication of
the body-frame**

The first step to determine the position of the gates was to identify the feasible areas, where the gate could be located on the part. Locating the gates on features subjected to high stress levels during operation is not recommended, as gates result in local stress concentrations. High stress areas were classified by:

- Functional stresses: Stresses appearing on the part during its regular operation;
- Demolding stresses: Stresses occurring during demolding of the part from the mold cavity.

Hence, placement of gates in these high stress locations is undesirable, since it would result in even higher stress levels in these areas. Therefore the feasible areas for the gate locations should be identified as regions that are not subjected to high stress levels. Once the feasible areas for the gate locations are identified, the next step involves determining the number of gates required to ensure appropriate part filling while managing warpage. In this step, the gates can be initially placed symmetrically within the part region containing the allowable gate locations. Filling simulations in Moldflow Plastics Insight reveal the effect of the gates on the part filling. However, the gate positions identified for appropriate mold filling may not ensure appropriate positions of weld-lines in the part. Hence, the next step involves positioning the gates such that the weld-line locations are acceptable. Weld-lines should not be located at areas which could potentially be exposed to high stresses.
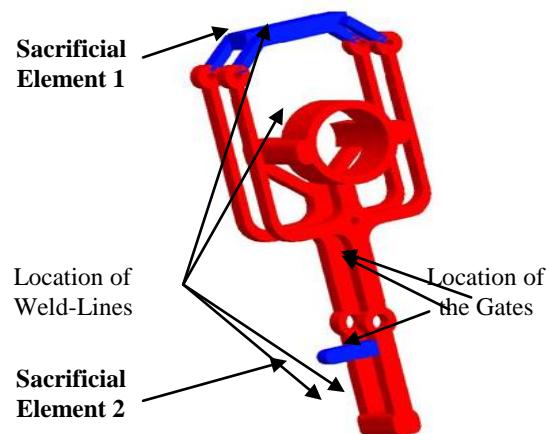

Figure 9.7: Sacrificial elements for absorbing weld-lines

Therefore the gates needed to be moved to more appropriate regions to ensure proper weld-line locations. However, some situations may necessitate addition of a gate to alter the weld-line locations. While moving or adding the gates, it is important to ensure that the part filling is not adversely affected by the new gate positioning. Adding or repositioning the gates may not be sufficient to eliminate all the weld-lines that result from the part molding. Hence, a sacrificial shape element may have to be added to absorb the weld-lines occurring in the critical areas. The overall approach used for gate positioning and sacrificial shape element design to absorb weld-lines was outlined in [21]. Using this approach, the gate positioning problem was solved for the body-frame. Finally, using this approach, the sacrificial elements needed for appropriate molding of the mechanism frame were determined. The final gate placement and sacrificial structure design is illustrated in Figure 9.7.

9.3.4 Results

The drive mechanism parts were molded on a Milacron Babyplast injection molding machine using HIVAL ABS HG6.

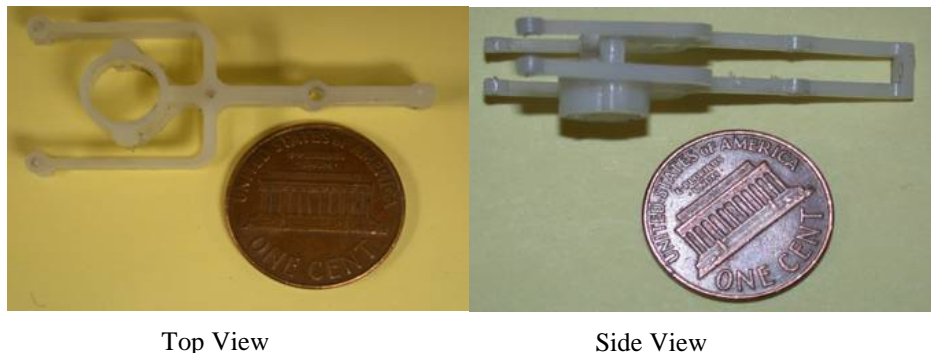Top View   Side View

Figure 9.8: In-mold fabricated body-frame

Figure 9.8 shows the photograph of the part manufactured using the molding strategy discussed in the previous section. Careful visual inspection of the part revealed that the weld-line was present at the predicted location, illustrated in Figure 9.7. After successfully accomplishing the molding of the drive frame, the rocker and wing supports of the mechanism were also injection molded.

Finally, the MAV was assembled using the molded parts, the gears, and the electronics. The Small Bird MAV designed and developed in the Advanced Manufacturing Laboratory is illustrated in Figure 9.9. The MAV was hand-launched and was capable of holding a sustained flight with controlled ascent and

descent. The authors were able to successfully steer and land the MAV indoors. The main performance specifications are listed in Table 9.1. Video of a successful flight can be found at http://terpconnect.umd.edu/~skgupta/UMdBird/
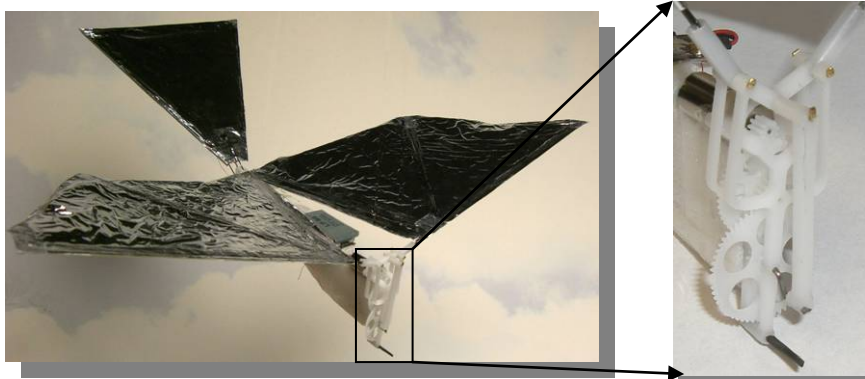

Figure 9.9: Small Bird MAV assembly

Table 9.1: Performance attributes of the Small Bird MAV

Overall Max. Weight	15.4 g
Payload Capability	5.7 g
Max. Flapping Frequency	12.1 Hz
Flight Duration	5 min
Flight Velocity	4.4 m/s

9.4   Case Study 2: Design of the Jumbo Bird

In this case study the focus was on developing a platform which had a significantly higher payload capacity. The payload capacity translates directly into the weight of sensors and batteries that can be carried onboard the MAV, substantially increasing its practical application to various missions. This section will present the approach to design the Jumbo Bird MAV transmission mechanism.
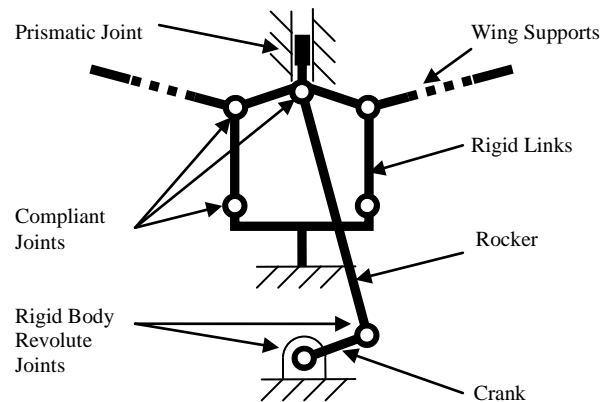

Figure 9.10: Jumbo Bird drive mechanism concept

In the previous case study, development of a small MAV, capable of successful and steerable flight, was presented. The transmission mechanism utilized geometrically distributed compliance; however, with increasing size of the MAVs, mechanisms with distributed compliance exhibit excessive deformations. Therefore localized compliance in the mechanism becomes a more attractive option, due to design scalability, and compactness of the assembly.

Figure 9.10 shows the schematic diagram of the mechanism concept. Several flexural joints were incorporated into the mechanism to provide for a local (lumped) compliance in the structure to facilitate motion. To enforce the synchronization of the wing motions, a prismatic joint was introduced.

9.4.1   Mechanism Shape Synthesis

The first step in the design framework outlined in Figure 9.1 was to perform the shape synthesis of the MAV transmission mechanism. This included the development of the basic mechanism geometry from the concept illustrated in

Figure 9.10, as well as identification of interlocking features on miniature compliant joints to achieve successful interconnection with the rigid links in a multi-material structure. Towards this end, the shape synthesis of the mechanism was carried out using the following three step approach. First, to generate a basic shape of the mechanism, the design concept was detailed by adding functionality and manufacturability constraints. Second, the constrained dimensions of the mechanism were determined by analyzing the mating components and motion requirements. Third, the miniature compliant joint geometry, necessary to achieve successful connection between incompatible polymers in a multi-material structure, was investigated.

The primary functional requirement for the MAV drive mechanism was to provide a synchronized flapping action of both wings. Importance of synchronization is emphasized, because it not only ensures the required flapping action for a successful flight of the MAV, but also contributes to the overall stability and efficiency of the mechanism. The flapping range was determined to be 65° [21]. Preliminary tests indicated that the flapping frequency of 4 to 6 Hz was required to sustain the flight.

To achieve flapping wing motion from the rotary input of the motor, a crank-rocker mechanism, based on the concept illustrated in Figure 9.10, was designed. The motor's rotational velocity was transferred to the crank through a gearbox to obtain the required flapping frequency. The crank was connected to a rocker, which displaced the symmetrically placed wing arms. These arms were pivoted on supporting members, which allowed for the displacement of the pivoting point by utilization of a lumped compliance. To ensure symmetry in the flapping motion, a prismatic joint was introduced at the point where rocker transferred the energy to the wing arms. This was crucial to the amount of thrust produced by the wings of the MAV. Figure 9.11 shows the developed mechanism design with characteristic features highlighted.
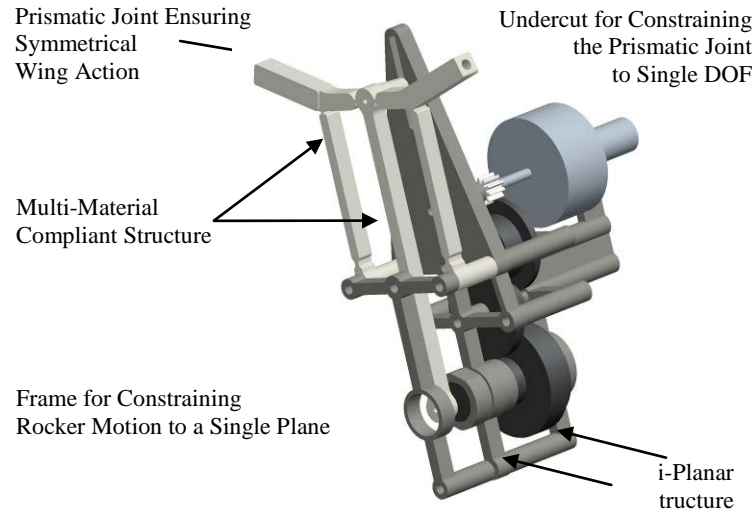
Prismatic Joint Ensuring
Symmetrical
Wing Action

Undercut for Constraining
the Prismatic Joint
to Single DOF

Multi-Material
Compliant Structure

Frame for Constraining
Rocker Motion to a Single Plane

i-Planar
tructure

Figure 9.11: Jumbo Bird drive mechanism design

The experimental results showed that disturbance forces can cause significant out of plane motion of the rocker and the wing arms. To eliminate these issues, an additional frame was designed for physical constraint of the rocker motion to a single plane, and an undercut feature on the back of the prismatic joint was added to constrain its motion to only one degree of freedom. This is illustrated in Figure 9.11.

In order to reduce the rotational velocity of the motor to match the flapping frequency requirement, a three-step gear reduction was designed. The gearbox utilized a bi-planar design. This allowed for two-point support of the gear axis, and allowed for prevention of the crank wobbling effect, induced by the torque transmission to the rocker. The bi-planar gearbox assembled with the frame constraining the rocker created a rigid tri-planar enclosure of the mechanism, preventing it from damage during MAV landing.

The drive mechanism utilized a multi-material compliant structure to transform the motor's rotational velocity to the flapping motion. This novel design combined seven rigid links connected with six compliant hinges to create a functional, single-piece mechanism. The molded structure consisted of the rocker, wing arms, and their supports. It also provided for the prismatic joint attachment point and a proper offset with respect to the crank.

In order to ensure the moldability of the multi-material compliant mechanism, fillets around the compliant joints were introduced to minimize the differences in the cavity cross-section and allow for robust hinge encapsulation in the rigid structure.

After identifying the basic shape of the mechanism using the functionality and moldability constraints, the next step is to determine the dimensions of the mechanism. Considering the functional requirements and constraints on the overall size of the MAV, it is important to first identify the constrained and free dimensions of the mechanism design. The constrained dimensions were identified from the functional requirements of the MAV.

The design of the mechanism required the rocker operational envelope to be placed between the wing arm supports. Therefore the minimum separation between the supporting members was constrained to 19 mm. For the required flapping range of 65°, the relative angle on the wing arms was designed to be 15°, and the length of the crank and the rocker to be 4.1 mm and 45.7 mm, respectively. The range of flapping motion also determined the range for the prismatic joint to be at least 12 mm, to account for elastic deformations of the structure in operation due to loading. The gear axis separation and the range of motion for the prismatic joint determined the minimum length of the mechanism to be 66 mm.

Moldability constraints of the compliant mechanism frame required that the main parting direction of the mold had to be perpendicular to the frame plane. Therefore the minimum thickness of the compliant joints was set to be 0.8 mm. The fixed dimensions of the mechanism based on the constraints described above are illustrated in Figure 9.12.
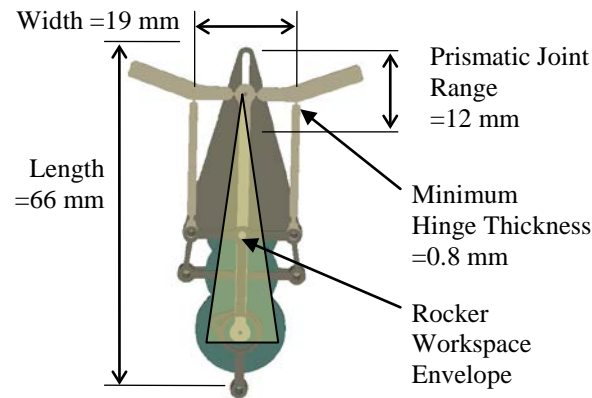

Figure 9.12: Constrained dimensions of the design

9.4.2 *Parametric Optimization*

The next step in the approach outlined in Figure 9.1 was to develop models to allow for design optimization of the multi-material compliant drive mechanism

of the MAV. To this end, the parametric models of the mechanism resulting from unconstrained dimensions developed in the previous section were employed and the experimental data was used as the boundary conditions in design evaluation simulation. Since the overall functionality of the MAV depends on its payload capabilities, the weight of the drive mechanism should be minimized with constraints set on load transfer capabilities required by a specific application. The design variables used included sizing of the mechanism rigid links, critical for the drive functionality, as well as sizing dimensions of the miniature compliant joint cross-section. The experimental results of lift and thrust forces generated by MAV wings were inserted into a dynamic simulation model as input boundary conditions. The simulation was used to estimate propagation of the wing forces through the mechanism structure. The results were inputted into a finite element analysis software to calculate stresses and strains on the structure. To minimize the weight of the mechanism without risking its failure, parts were sized to achieve the required factor of safety.

Design optimization of the mechanism required knowledge of the forces acting on links and joints. Lift and thrust forces generated by the wings were measured experimentally [20]. The measured average thrust was 0.384 N, with peak amplitude of 1.724 N. Thrust values were recorded using a stationary platform without any external air stream. The measured average lift was 0.591 N, with the peak amplitude of 1.862 N. Lift values were recorded using a wind tunnel with a moving air stream to simulate the flight conditions.

Since the wings were mounted to the body of the MAV at both front and rear, only a fraction of the forces measured by the load cell were actually transmitted to the mechanism parts. To measure the force distribution over the wing mounting points, a small deflection frame was attached to the back of the wings. The frame deformations were optically measured and the forces were calculated from the deflections. Subtracting the forces observed as deflections on the frame from the total load cell measurements yielded the actual forces experienced by the mechanism.

The simulation of wing forces' propagation onto the mechanism parts was performed using a planar dynamics model. Due to the low operating frequency of the mechanism, and a relatively low mass of the moving components, the weights of the mechanism moving parts were observed negligible. Therefore the inertial effects of the mechanism were ignored.

The mechanism was modeled using MSC Adams View R3 software. The model was used to analyze the distribution of reaction forces. Static equilibrium simulation for two full wing flap cycles was performed. Static cases were obtained, where the combined load on the structure induced the highest von Mises stresses. The most demanding and prone to failure mechanism components were identified as the rocker element and the wing arms. The most demanding hinges were present at the point where the rocker connects to the wing arms. The data points with the greatest magnitude of combined loading

during the flapping cycle were chosen as inputs to the analysis, such that the factor of safety would correspond to the worst case scenario loading of the design.

After constraining the dimensional parameters of the mechanism to accommodate mechanical and electronic components required for the functionality of the MAV, the remaining mechanism dimensions had to be determined, namely the rocker thickness, wing arms' thickness, and the compliant hinge cross-section. These were assigned by a finite element analysis-based design optimization. The goal of the optimization was to minimize the weight of the mechanism, while satisfying the manufacturability and maximum allowable stresses constraints.

The von Mises stresses in the mechanism were found from the worst case loading scenarios. The loading conditions found to induce the largest stresses in the mechanism were applied to the corresponding points on the 3D mechanism model.

The finite element analysis was performed using the Mechanica module of Pro/Engineer Wildfire 4.0 software. The analysis of the worst case loading scenario was performed and the maximum von Mises stresses were plotted across the structure. The yield strength of the material was then divided by the peak stress to determine the resulting factor of safety. The value of the factor of safety was designed similarly to the first case study; however the value was increased to be 2.0 due to the higher uncertainties associated with the use of composite material. Hence, the required cross-section dimensions of the rocker were found to be 2.1 x 2.5 mm, and of the wing arms to be 2.5 x5.1 mm. Similarly, the hinge cross-section dimensions were obtained. To allow for low-energy bending, the thickness of the hinge was determined to be 0.9 mm. Considering the forces transmitted by the miniature hinges from the rocker, the depth of the hinge was calculated to be 5.1 mm.

9.4.3   Manufacturability Analysis

This section will describe the development of a manufacturing process to create multi-material compliant mechanisms. This process was developed using the cavity transfer method. Additional considerations were given to the miniature scale involved.

The choice of a specific multi-material molding (MMM) method to realize compliant structures with miniature hinges is a trade-off between the mold complexity and cycle time. Several morphing cavity methods have been developed [17], offering a high level of automation. Due to the fact that morphing cavity methods need to allow for disassembly of the mold pieces, the complexity of the part shape drastically affects the complexity of the molds. Hence, the tooling cost and lead times are significantly increased. To reduce the mold complexity while maintaining the generality of the manufacturing approach, the cavity transfer method [22] was employed in this case study. Optimum mold design consists of minimum number of mold pieces. The chosen cavity transfer

method resulted in a minimum number of two mold pieces for each of the molding stages.

The process sequence developed to manufacture multi-material compliant MAV drive mechanism is presented in Figure 9.13. The first stage involved molding miniature hinges for realizing articulating joints in the mechanism. Demolded first stage components were then transferred to the second stage mold cavity. After the mold closing, the second stage fiber-enhanced polymer was injected into the multiple cavities to create the rigid links of the mechanism structure. Note that this step was an automated assembly operation, which took place directly inside the mold during the second stage molding. The compliant structure was then demolded and was ready to be assembled with the mechanism gearbox and the wings.

Gate type and location are always important design variables in injection mold design, as they largely affect the cavity fill patterns. Improper choice of gate type and location induces unbalanced flow, which causes overpacking, high shear stress, and excessive warpage. The gate position also induces the fiber orientation for the filled polymers, influencing the properties of the molded part. Therefore gate placement is of a great importance to achieve high quality products with required properties. Optimum gating will ensure the required structural properties of the product and will allow for easy demolding operation.
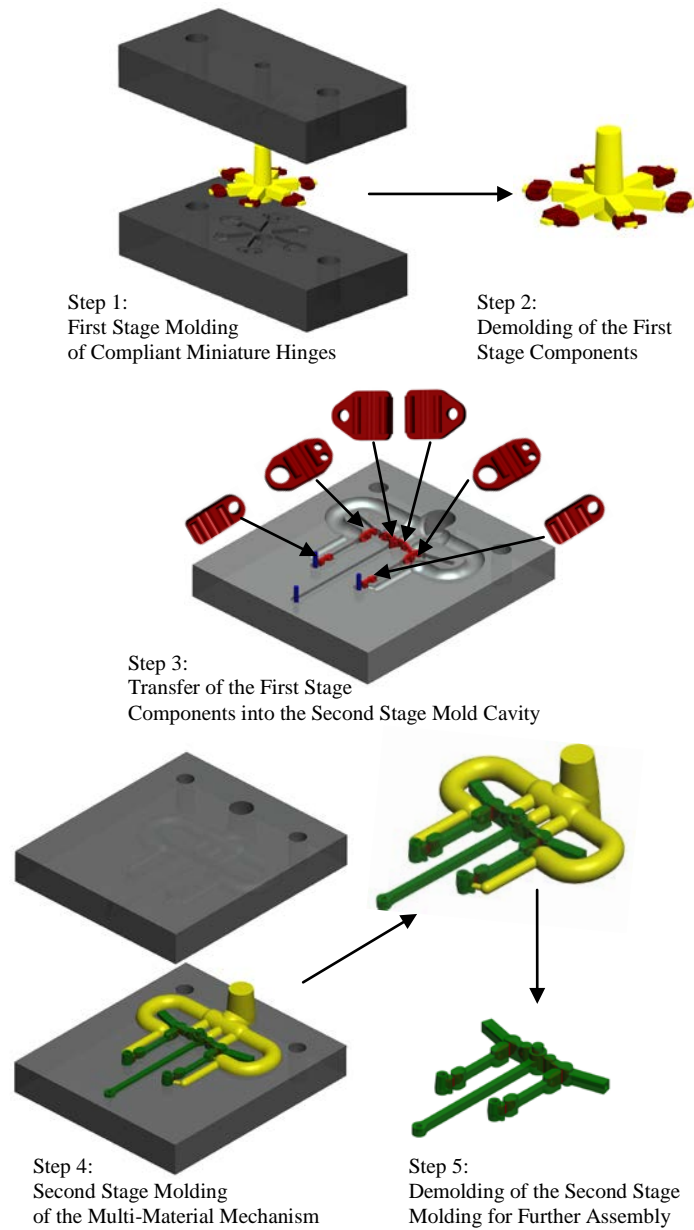
Step 1:
First Stage Molding
of Compliant Miniature Hinges

Step 2:
Demolding of the First
Stage Components

Step 3:
Transfer of the First Stage
Components into the Second Stage Mold Cavity

Step 4:
Second Stage Molding
of the Multi-Material Mechanism

Step 5:
Demolding of the Second Stage
Molding for Further Assembly

Figure 9.13: Overview of the developed MMM process

In the first stage of the process, compliant hinges were molded. To ensure long life of the hinge, the polymer chains should be oriented perpendicular to the hinge as they cross it. Therefore film gates were used to provide for a flow front

progression aligned with the flexural axis of the joint. Additionally, sacrificial features were added on the part. These served two separate functions: 1) As an extension of the gate, they allowed for a desired flow pattern along the whole length of the hinge, and 2) They allowed for an easy demolding operation, without the risk of damaging the miniature components. The gate and sacrificial feature of the first stage molding are shown in Figure 9.14(a).
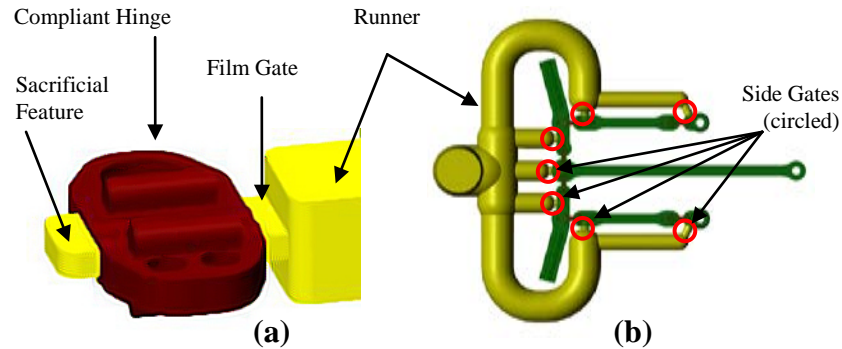

Figure 9.14: Gate designs used in the MMM process: (a) first-stage film gate, and (b) second-stage side gate layout.

In the second stage of the process, the multi-material mechanism frame was created by molding the rigid links over the first stage compliant hinges. Considering the functional requirements of the design, a glass fiber filled polymer composite was used to enhance the load transfer capabilities of the rigid links in the mechanism. However, properties of filled polymer moldings are very dependent on the filler orientation across the part. Since the filling pattern inside the cavity is a strong function of the gate position, the gate positions had to be carefully designed to result in parts that fully utilize the enhanced material properties. Due to weight limitations in MAV applications, the volume of drive mechanism links needed to be minimized, which resulted in several elongated cavities in the second stage mold. Since the filler particles tend to get aligned with the polymer flow during the cavity filling phase, the side gate positions in these cavities were determined to lie on one of the ends, such that the resulting runner layout would have the minimum number of relatively long channels. This gate layout was evaluated using mold filling simulation to ensure uniform orthotropic properties of the mechanism links molded from the glass fiber reinforced polymer. The gates were sized according to common injection molding guidelines [10]. The gate layout in the second stage molding is shown in Figure 9.14 (b).

The primary function of the runner system in injection molds is to supply the mold cavities with a molten polymer from the injection nozzle. Realizing multi-material compliant mechanisms with MMM process requires a specific runner layout design. Molding the second stage components over the first stage parts results in the cavity separation, and hence, multi-cavity molds. Each of these cavities needs a separate supplying runner. Since the cavity layout is determined by the mechanism functional design, and the gate positions for each cavity are often fixed, as described above, the main design objective for the runner system is to provide for a complete mold filling. Additionally, to provide for a strong encapsulation of the first stage moldings in the second stage parts, the second stage polymer flows should arrive at the pre-molded component from adjacent cavities in roughly the same amount of time. This is required for: 1) Minimization of highly directional forces which may be induced on the mold insert by an unbalanced flow pattern, resulting in the insert's displacement and failed molding, and 2) Strength improvement of the weld-line, formed when the second stage polymer flows around the first stage component. This is due to the fact that the weld-line strength increases with the temperature of the weld-line formation. Moreover, the polymer which solidifies inside the runner cavity is treated as production waste after demolding; therefore the volume of the runner system should be minimized.

9.4.4   Results

A multi-material compliant frame for the Jumbo Bird MAV drive mechanism was molded on a Milacron Babyplast injection molding machine. LDPE was used in molding the first stage components – compliant joint inserts. Short glass fiber-filled (15% vol.) Nylon 6,6 was used in the second stage molding to create the rigid links of a multi-material compliant structure. Delrin® was used for manufacturing the crank, motor holder, and the gearbox frame for the mechanism.

Figure 9.15 shows the photograph of the multi-material molding of the compliant MAV drive frame manufactured using the cavity transfer method described in the previous sub-section. Careful visual inspection of the demolded part revealed no molding defects such as deep weld-lines, excessive warpage, or displaced compliant joints.

After successfully molding the multi-material compliant drive frame, the mechanism was assembled using the molded and machined parts, along with off-shelf components, including gears, rods, and motor. The MAV body consisted of the drive mechanism, with wings attached on the front, and the tail servo-motor at the back, both connected with two carbon fiber rods and a foam body. The foam body served as housing for the motor speed controller and the remote control receiver, as well as the rear anchoring point for the wings.
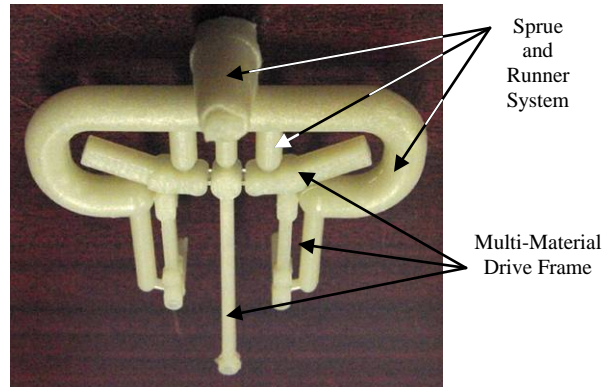
Figure 9.15: Multi-material molding of MAV drive frame

A brushless motor was chosen to actuate the mechanism, because of its high efficiency and low weight. Then, the electronic components required for powering and controlling the MAV were matched from the lightest market-available options. These included the speed controller for the motor, the remote control receiver, the tail actuator and the battery cell. The assembly of the MAV is shown in Figure 9.16.
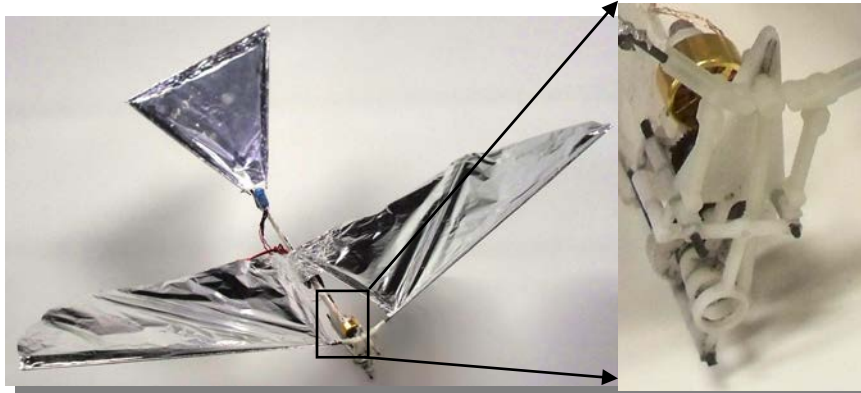

Figure 9. 16: Jumbo Bird MAV assembly

The Jumbo Bird MAV designed and developed in the Advanced Manufacturing Laboratory was capable of: 1) A remote launch from a four-wheel RC vehicle, 2) Holding a sustained outdoor flight with controlled ascent, descent,

and steering, and 3) Controlled landing in a safe area. The main performance specifications are listed in Table 9.2. Video of the successful indoor and outdoor flights can be found at: http://terpconnect.umd.edu/~skgupta/UMdBird/

Table 9. 2: Performance attributes of the Jumbo Bird MAV

Overall Max. Weight	71.0 g
Payload Capacity	33.0 g
Max. Flapping Frequency	6.1 Hz
Flight Duration	15 min
Flight Velocity	3.04 m/s

9.5   Conclusions

This chapter presented a modeling and simulation based approach required for the design and fabrication of MAV drive mechanisms. The overall framework of the design approach outlined in this chapter incorporates the advances in modeling and simulations methods in kinematic and dynamic analysis, finite element analysis and manufacturability analysis. Designers can use the methods presented in this chapter to design a flapping wing MAV drive mechanisms of any size using different energy sources and actuation elements.

Case studies of two different MAV drive mechanisms have been presented, which utilize the general design framework that has been described in this chapter. These drive mechanisms have been used in two different MAVs, differing significantly in weight and payload capabilities. The technical feasibility of both mechanism designs have been demonstrated through successful test flights of the MAVs. The drive mechanisms have been optimized for the performance of the MAV and their payload capacities. The Small Bird MAV was capable of a sustained flight with a maximum payload capacity of 5.7 grams (59% of total unloaded MAV weight). The Jumbo Bird MAV, on the other hand, was capable of carrying a 33 gram payload (87% of the total unloaded MAV weight). While airborne, the small bird performed very well in indoor conditions. The Jumbo Bird was found to be highly stable and controllable in both indoor and outdoor flights.

9.6   Acknowledgements

9.7   References

1. C. Galinski, and R. Zbikowski. Materials challenges in the design of an insect-like flapping wing mechanism based on a four-bar linkage. Materials & Design, Vol. 28 (3): pp. 783-796, 2007.
2. R. Madangopal, Z.A. Khan, and S.K. Agrawal. Biologically inspired design of small flapping wing air vehicles using four-bar mechanisms and quasi-steady aerodynamics. Journal of Mechanical Design, Vol. 127 (4): pp. 809-816, 2005.
3. T. Tantanawat, and S. Kota. Design of compliant mechanisms in minimizing input power in dynamic applications. Journal of Mechanical Design, Vol. 129 (10): pp. 1064-1075, 2007.

4. P. Zdunich, D. Bilyk, M. MacMaster, D. Loewen, J. DeLaurier, R. Kornbluh, T. Low, S. Stanford, and D. Holeman. Development and testing of the Mentor flapping-wing micro air vehicle. Journal of Aircraft, Vol. 44 (5): pp. 1701-1711, 2007.

5. A. Cox, D. Monopoli, D. Cveticanin, M. Goldfarb, and E. Garcia. The development of elastodynamic components for piezoelectrically actuated flapping micro-air vehicles. Journal of Intelligent Material Systems and Structures, Vol. 13 (9): pp. 611-615, 2002.

6. S.K. Banala, and S.K. Agrawal. Design and optimization of a mechanism for out-of-plane insect wing-like motion with twist. Journal of Mechanical Design, Vol. 127 (4): pp. 841-844, 2005.

7. L.L. Howell. Compliant mechanisms. Wiley-Interscience, 2001.

8. N.D. Mankame, and G.K. Ananthasuresh. A novel compliant mechanism for converting reciprocating translation into enclosing curved paths. Journal of Mechanical Design, Vol. 126 (4): pp. 667-672, 2004.

9. H. Zhou, and K. Ting. Shape and size synthesis of compliant mechanisms using wide curve theory. Journal of Mechanical Design, Vol. 128 (3): pp. 551-558, 2006.

10. J.P. Beaumont. Runner and gating design handbook: Tools for successful injection molding. Hanser Gardner Publications, 2004.

11. J.P. Beaumont, R. Nagel, and R. Sherman. Successful injection molding: Process, design, and simulation. Hanser Gardner Publications, 2002.

12. J.Y.H. Fuh, Y.F. Zhang, A.Y.C. Nee, and M.W. Fu. Computer aided injection mold design. Marcel Dekker Inc., 2004.

13. D.O. Kazmer. Injection mold design engineering. Hanser Gardner Publications, 2007.

14. M.J. Madou. Fundamentals of microfabrication. CRC Press, 2002.

15. R.A. Malloy. Part design for injection molding. Hanser Gardner Publications, 1994.

16. G. Menges, W. Michaeli, and P. Mohren. How to make injection molds. Hanser Gardner Publications, 2001.

17. A.K. Priyadarshi, S.K. Gupta, R. Gouker, F. Krebs, M. Shroeder, and S. Warth. Manufacturing multi-material articulated plastic products using in-mold assembly. International Journal of Advanced Manufacturing Technology, Vol. 32 (3-4): pp. 350-365, 2007.

18. C. Fetecau, and F. Stan. Computational prediction of defects during injection molding in a complex part. Materiale Plastice, Vol. 44 (3): pp. 180-184, 2007.

19. C.H. Wu, and W.J. Liang. Effects of geometry and injection molding parameters on weld-line strength. Polymer Engineering and Science, Vol. 45 (7): pp. 1021-1030, 2005.

20. D. Mueller, H.A. Bruck, and S.K. Gupta. Measurement of thrust and lift forces associated with drag of compliant flapping wing for micro air vehicles using a new test stand design. Experimental Mechanics, 50(6):725–735, 2010.

21. W. Bejgerowski, A. Ananthanarayanan, D. Mueller, and S.K. Gupta. Integrated product and process design for a flapping wing drive mechanism. Journal of Mechanical Design, Vol. 131 (6): pp. 061006, 2009.

22. R.M. Gouker, S.K. Gupta, H.A. Bruck, and T. Holzschuh. Manufacturing of multi-material compliant mechanisms using multi-material molding. International Journal of Advanced Manufacturing Technology, 3011-12): 1049-1075, 2006.